Substrate Integrated Waveguide Horn Antenna on Thin Substrate With Back-Lobe Suppression and Its Application to Arrays

Yu Luo, *Member, IEEE*, and Jens Bornemann, *Fellow, IEEE*

***Abstract*—A substrate integrated waveguide H-plane horn antenna on thin substrate with low back-lobe radiation is presented, and its application to arrays demonstrated. To suppress the back lobe, a pair of slots is employed in the top and bottom metallization. After size and position of the pair of slots are investigated, low back-lobe radiation is achieved. Moreover, the size of the horn aperture is approximately one wavelength, which is suitable for array applications. To highlight this point, the proposed horn antenna is used in a 1×4 planar array on a substrate as thin as one tenth of the wavelength. The array is designed, fabricated, and measured. Measurements show good agreement with simulations and suppressed back-lobe radiation with a 24 dB front-to-back ratio.**

***Index Terms*—Array, back-lobe, horn antenna, substrate integrated waveguide (SIW).**

I. Introduction

SUBSTRATE integrated waveguide (SIW) H-plane horn antennas, as one kind of typically planar horn antennas, exhibit attractive advantages of low profile, simple fabrication, and easy integration with other components [1]. However, the low back-lobe performance of planar horn antennas diminishes significantly when the substrate thickness is much smaller than the free-space wavelength, λ_0 [2]–[4]. To alleviate the aperture-radiated waves, which contribute to antenna back radiation, different kinds of structures [5]–[10] are employed in front of the aperture. However, the additions of such structures significantly enlarge the size of the entire antenna. To suppress undesired back radiation, planar strips on soft surfaces are attached to the top and bottom of the substrate integrated horn [11], but it results in a multilayer structure. Perforating air-vias with different diameters are employed in [12] to suppress the back lobe and improve the bandwidth and reflection coefficient of the horn. Unfortunately, the substrate is as thick as 0.32 λ_0, which increases difficulties in fabrications. Strip-via arrays are employed at the side of an air-filled horn to obtain a low back lobe [13], but it requires a multilayer structure. Most importantly, all the apertures in [5]–[13] are much wider than the corresponding free-space wavelengths, which render them unsuitable for many array applications that require spacing of approximately 1 λ_0. Some SIW horn arrays are proposed in [5], but the dimensions of elements in the array are different from the ones of a single element, and the back-lobe performances of the arrays are not mentioned in the paper.

Therefore, in this letter, a back-lobe suppressed SIW H-plane horn antenna on thin substrate and its application to arrays are presented. To suppress the back radiation, a pair of slots is employed behind the aperture in the top and bottom metallization. The positions and sizes of the slots are investigated to provide a guideline for placing such slots. To demonstrate that the proposed antenna is suitable for array applications, an array formed with the proposed antenna is designed, fabricated, and measured.

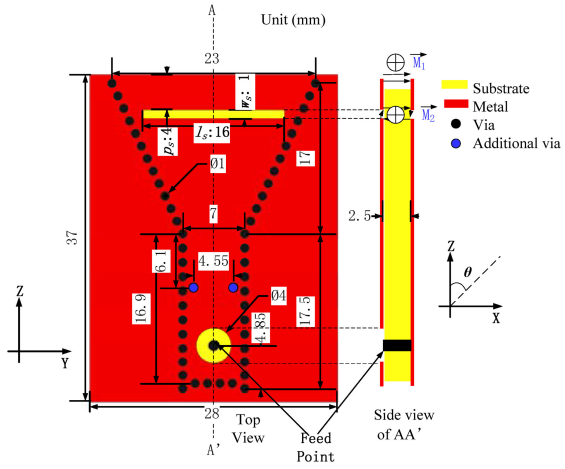

Fig. 1. Top and side views of the proposed SIW horn antenna with a pair of slots and its dimensions.

II. Back-Lobe Suppressed SIW Horn Antenna on Thin Substrate

The layout of the SIW H-plane horn antenna with low back-lobe radiation is shown in Fig. 1. The substrate is Rogers 6006 with thickness of 2.5 mm (0.1 λ_0) and $\varepsilon_r = 6.15$.

To satisfy array application requirements, the aperture width is selected as one wavelength at center frequency. To suppress back radiation, a pair of slots is employed in both top and bottom

Manuscript received June 6, 2017; revised August 1, 2017; accepted August 1, 2017. Date of publication August 7, 2017; date of current version September 18, 2017. This work was supported by the National Science and Engineering Research Council of Canada. *(Corresponding author: Jens Bornemann.)*

Y. Luo was with the Department of Electrical and Computer Engineering, University of Victoria, Victoria, BC V8W 2Y2, Canada. He is now with the Department of Electrical and Computer Engineering, National University of Singapore, Singapore 117583 (e-mail: elelyu@nus.edu.sg).

J. Bornemann is with the Department of Electrical and Computer Engineering, University of Victoria, Victoria, BC V8W 2Y2, Canada (e-mail: j.bornemann@ieee.org).

Color versions of one or more of the figures in this letter are available online at http://ieeexplore.ieee.org.

Digital Object Identifier 10.1109/LAWP.2017.2736445

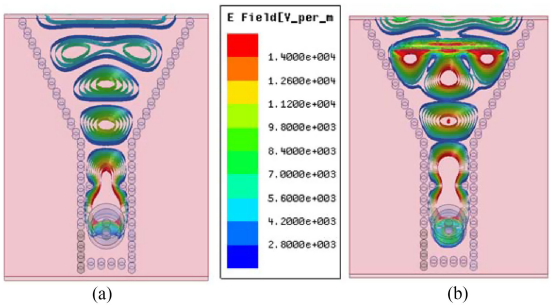

Fig. 2. Complex magnitude *E*-field distributions of the horn with or without slots. (a) Without slots. (b) With slots.

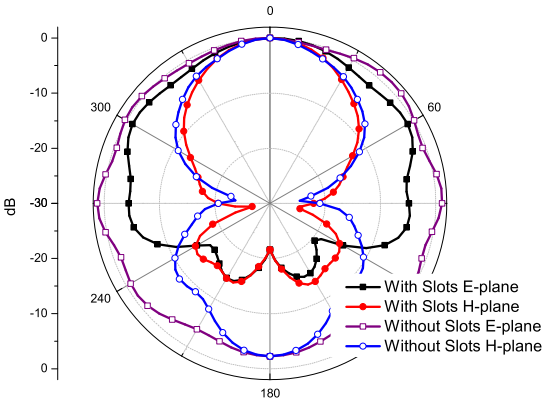

Fig. 3. Effect of the slots on radiation patterns at 12.4 GHz.

surfaces. The length of the slots is set as l_s, their width as w_s, and their position, i.e., the distance between the aperture and the slots, as p_s. The aperture can be treated as magnetic current $\vec{M}_1$, and the pair of radiating slots as $\vec{M}_2$. The radiation pattern $f(\theta)$ of the two magnetic currents in the xz plane can be calculated as:

$$f(\theta) = \vec{M}_1 e^{-j\frac{kp_s}{2}\sin\theta} g_1(\theta) + \vec{M}_2 g_2(\theta) \quad (1)$$

where $g_i(\theta)$ is the radiation pattern of the ith magnetic current, and $k = 2\pi/\lambda_0$ is the wavenumber.

If the radiations of $\vec{M}_1$ and $\vec{M}_2$ toward the back direction, i.e., in negative z-direction (see Fig. 1), have the same magnitude and opposite phase, low back-lobe radiation can be realized. The complex magnitude *E*-field distributions of the horn with and without slots are shown in Fig. 2. Without the slots, only the aperture radiates the power. With the addition of the slots, the aperture and the slots radiate power together. If the position and size of the slots is well selected, the back radiation of the aperture and that of the slots can cancel each other. The effect of the addition of the two slots on the radiation pattern is shown in Fig. 3. Without slots, the front-to-back radio is only 2.8 dB. After the addition of slots to the 0.1 λ_0 thin substrate, as predicted, the front-to-back ratio is increased from 2.2 to 21.6 dB, and low back radiation is obtained. Note that the influence of the slots on the E-plane pattern is such that it slightly reduces the E-plane beamwidth due to the improved front-to-back ratio.

To understand the effects of the slots on the back radiation, the three critical parameters p_s, w_s, and l_s are investigated.

The first parameter studied is p_s as shown in Fig. 4. The position of the slots mainly affects the phase difference between the two magnetic currents in (1). With p_s increasing from 3 to 4 mm, the front-to-back ratio is enhanced from 1.6 to 21.6 dB and lowest back radiation is obtained. Beyond $p_s = 4$ mm, the back radiation becomes stronger again.

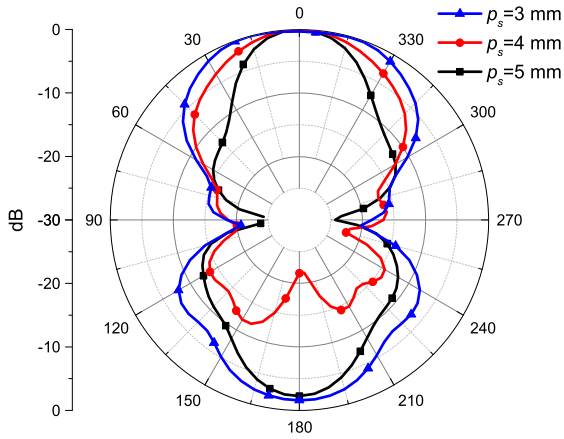

Fig. 4. Effect of p_s on H-plane (yz plane) radiation patterns at 12.4 GHz ($w_s = 1$ mm, $l_s = 16$ mm).

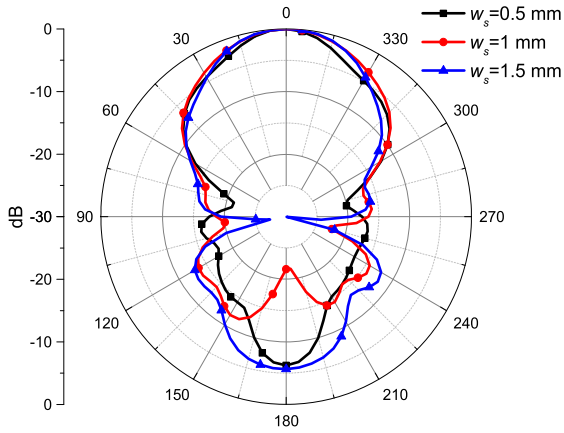

Fig. 5. Effect of w_s on H-plane (yz plane) radiation patterns at 12.4 GHz ($p_s = 4$ mm, $l_s = 16$ mm).

The second parameter investigated is w_s, and results are shown in Fig. 5. The width of the slots mainly affects the magnitude ratio of the two magnetic currents. When $w_s = 0.5$ mm, the magnitude of $\vec{M}_2$ is smaller than that of $\vec{M}_1$, and the front-to-back ratio is only 6.2 dB. When w_s increases from 0.5 to 1 mm, the magnitudes of the two magnetic currents become almost the same, and the highest front-to-back ratio of 21.6 dB is achieved. When w_s increases to 1.5 mm, the magnitude of $\vec{M}_2$ becomes larger than that of $\vec{M}_1$, and the front-to-back ratio decreases again to 5.6 dB.

As with the width w_s, the third parameter l_s also mainly affects the magnitude ratio of the two magnetic currents (see Fig. 6). When $l_s = 15$ mm, the magnitude of $\vec{M}_2$ is smaller than that of $\vec{M}_1$, and the front-to-back ratio is 16.6 dB. When $l_s = 16$ mm, the magnitudes of the two magnetic currents become almost identical, and the highest front-to-back ratio of about 21.6 dB is observed. Beyond $l_s = 16$ mm, the back lobe becomes larger again due to the increasing magnitude of $\vec{M}_2$.

In summary, to obtain the highest front-to-back ratio, $p_s = 4$ mm, $w_s = 1$ mm, and $l_s = 16$ mm are selected.

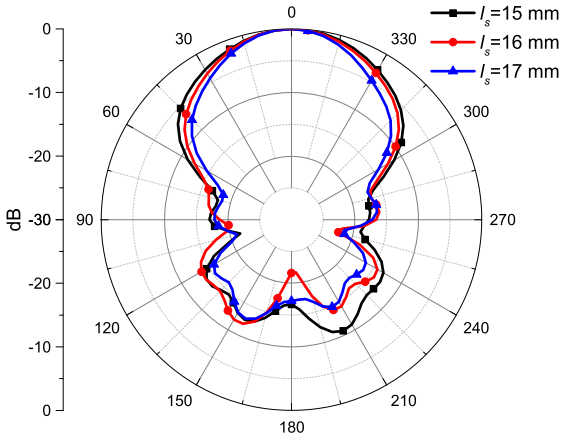

Fig. 6. Effect of l_s on H-plane (yz plane) radiation patterns at 12.4 GHz ($p_s = 4$ mm, $w_s = 1$ mm).

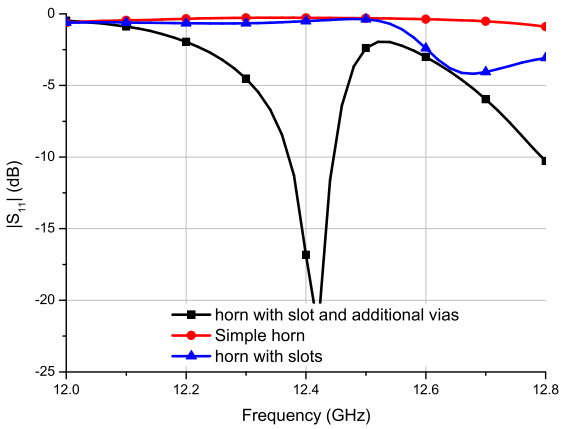

Fig. 7. Effect of slots and additional vias on $|S_{11}|$ of a single antenna.

Two additional vias (cf., Fig. 1) are employed in the waveguide and operate as a matching iris. With these additional vias, the return loss of the single element at 12. 4 GHz increases significantly as shown in Fig. 7. The reflection coefficients of the simple horn element (with and without slots) are also shown in Fig. 7. This indicates that the effect of the slots on $|S_{11}|$ is small.

III. Array Application

To demonstrate that the proposed SIW horn antenna is suitable for array applications on thin substrates with low back radiation, a 1×4 SIW antenna array is designed as shown in Fig. 8. It is fed by a 1-to-4 divider network whose dimensions are also shown in Fig. 8.

As discussed in Section II, four pairs of slots are employed to reduce back radiation. The dimensions of the horn elements, the size and position of slots, and the substrate are the same as those of the single element presented in Section II. The effects of the slots on the E- and H-plane radiation patterns are shown in Fig. 9. Without slots, strong back radiation is observed, and the front-to-back ratio is only 4.6 dB. With the slots, the back lobe is suppressed, and the front-to-back ratio is enhanced to 22.6 dB. Since the aperture is less than one wavelength, the side lobe level is only –13 dB.

Some vias are employed in the feeding network and operate as matching irises. With these additional vias, the bandwidth is

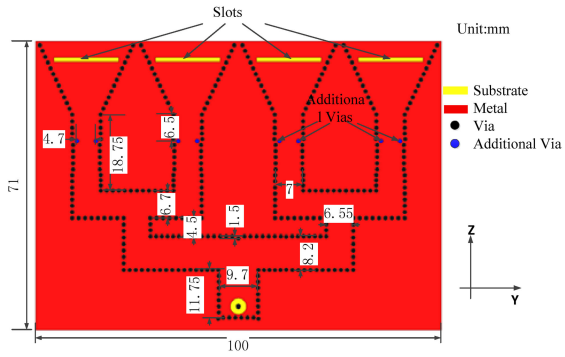

Fig. 8. Layout of the 1×4 SIW antenna array.

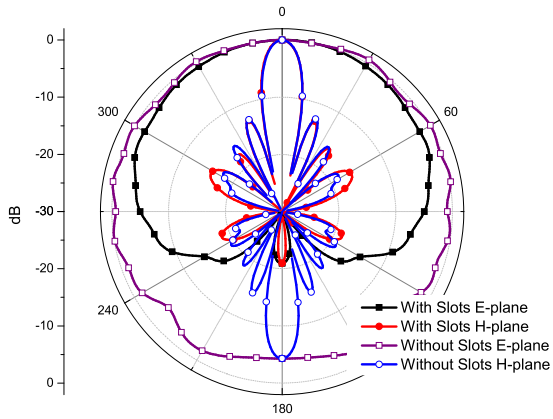

Fig. 9. Effects of slots on radiation patterns of the proposed 1×4 array at 12.4 GHz.

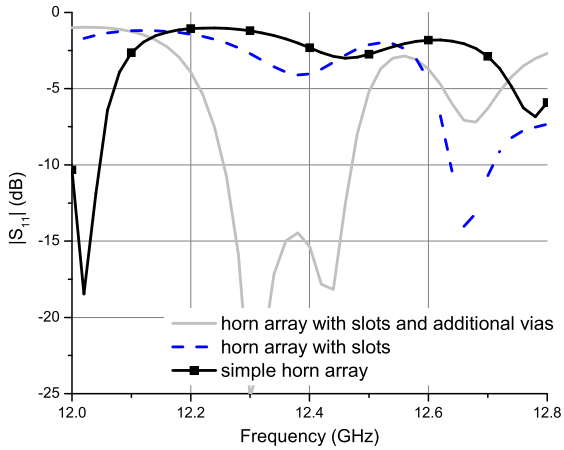

Fig. 10. Effect of slots and additional vias on $|S_{11}|$ of proposed 1×4 array.

enhanced as shown in Fig. 10. Without additional vias, the minimum $|S_{11}|$ around 12.4 GHz is only –3 dB. With the addition of the vias, $|S_{11}|$ is better than –10 dB in the frequency band from 12.25 to 12.47 GHz. The widths of the SIWs are also optimized for good impedance matching. The $|S_{11}|$ of the simple horn array is also exhibited in Fig. 10. This indicates that the effect of the slots on $|S_{11}|$ is small.

To verify the proposed design, the antenna array is fabricated and measured. Fig. 11 depicts a photograph of the fabricated prototype.

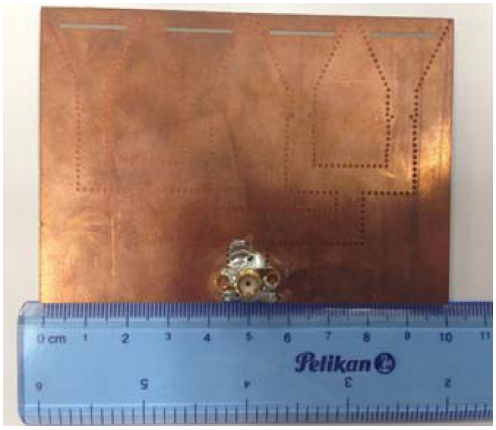

Fig. 11. Photograph of the proposed 1 × 4 SIW array.

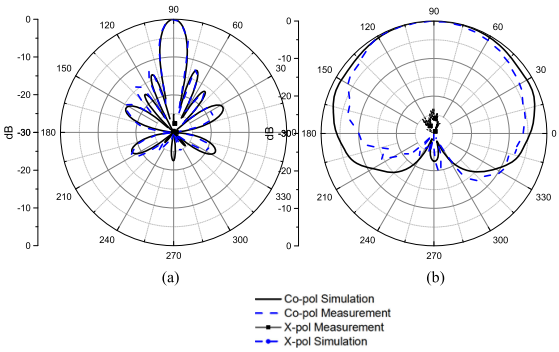

Fig. 12. Normalized simulated and measured radiation patterns of proposed 1 × 4 array at 12.4 GHz. (a) H-plane. (b) E-plane.

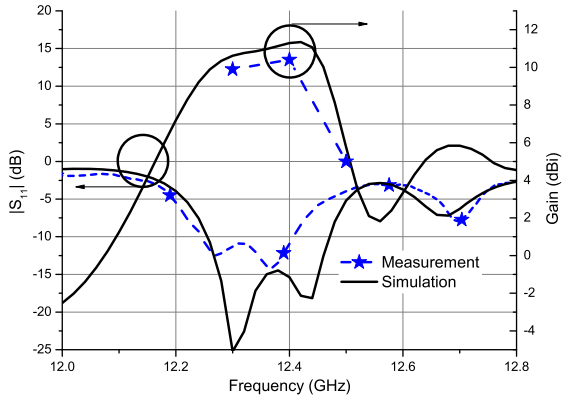

Fig. 13. Simulated and measured $|S_{11}|$ of proposed 1 × 4 array.

Measurements of the reflection coefficient, gain, and radiation patterns are performed using an Agilent 5230A vector network analyzer and a far-field antenna test chamber. The normalized simulated and measured radiation patterns are shown in Fig. 12. Good agreement between simulations and measurements is observed. As predicted, measured results show very low back-lobe radiation, and the front-to-back ratio is as high as 24 dB. In addition, the side lobe level is only –13 dB to prove that the proposed antenna is suitable for array applications. The measured gain, as shown in Fig. 13, at the center frequency, i.e., 12.4 GHz, is 10.4 dBi, which is slightly lower than the simulated one of 11.3 dBi. We attribute the difference of 0.9 dB to losses in the feeding SMA connector as well as other cable connections. The simulated and measured reflection coefficients as a function of frequency are also shown in Fig. 13. In the frequency band between 12.24 and 12.41 GHz (1.4% relative bandwidth), the measured reflection coefficient is better than –10 dB.

IV. Conclusion

An SIW H-plane horn antenna on thin substrate with low back radiation is presented. It is demonstrated that the front-to-back ratio can be significantly enhanced by the addition of a pair of slots in the top and bottom metallization. The proper size and position of the slots provide very low back radiation, which is sufficient for substrate integrated circuits on thin substrates. Since the aperture width of the horn is smaller than one wavelength, the proposed antenna is suitable for array applications. A prototyped 1×4 SIW horn antenna array shows 24 dB front-to-back ratio and side lobe levels better than –13 dB. To the best of our knowledge, this is the first time that an SIW horn antenna array with low back-lobe radiation on thin substrate is presented.

Acknowledgment

The authors would like to thank Prof. Z.-N. Chen of the National University of Singapore for his assistance with measurements.

References

[1] M. Bozzi, A. Georgiadis, and K. Wu, "Review of substrate-integrated waveguide circuits and antennas," *Microw. Antennas Propag.*, vol. 5, no. 8, pp. 909–920, Jun. 2011.

[2] M. Esquius-Morote, B. Fuchs, J. Zurcher, and J. R. Mosig, "A printed transition for matching improvement of SIW horn antennas," *IEEE Trans. Antennas Propag.*, vol. 61, no. 4, pp. 1923–1930, Apr. 2013.

[3] L. Wang, X. X. Yin, S. L. Li, H. X. Zhao, L. L. Liu, and M. Zhang, "Phase corrected substrate integrated waveguide H-plane horn antenna with embedded metal-via arrays," *IEEE Trans. Antennas Propag.*, vol. 62, no. 4, pp. 1854–1861, Apr. 2014.

[4] N. Bayat-Makou and A. A. Kishk, "Cavity matching of high dielectric constant SIW H-plane horn antenna," in *Proc. Int. Symp. IEEE Antennas Propag. USNC/URSI Nat. Radio Sci. Meet.*, Vancouver, BC, Canada, Jul. 2015, pp. 850–851.

[5] H. Wang, D.-G. Fang, B. Zhang, and W.-Q. Che, "Dielectric loaded substrate integrated waveguide (SIW) H-plane horn antennas," *IEEE Trans. Antennas Propag.*, vol. 58, no. 3, pp. 640–647, Mar. 2010.

[6] M. Esquius-Morote, B. Fuchs, J. Zurcher, and J. R. Mosig, "Novel thin and compact H-plane SIW horn antenna," *IEEE Trans. Antennas Propag.*, vol. 61, no. 6, pp. 2911–2920, Jun. 2013.

[7] N. Bayat-Makou, M. S. Sorkherize, and A. A. Kishk, "Substrate integrated horn antenna loaded with open parallel transitions," *IEEE Antennas Wireless Propag. Lett.*, vol. 16, pp. 349–351, 2017.

[8] Y. Cai *et al.*, "Compact wideband SIW horn antenna fed by elevated-CPW structure," *IEEE Trans. Antennas Propag.*, vol. 63, no. 10, pp. 4551–4557, Oct. 2015.

[9] L. Gong, K. Y. Chan, and R. Ramer, "Substrate integrated waveguide H-plane horn antenna with improved front-to back ratio and reduced side lobe level," *IEEE Antennas Wireless Propag. Lett.*, vol. 15, pp. 1835–1838, 2016.

[10] Y. Zhao, Z. Shen, and W. Wu, "Wideband and low-profile H-plane ridged SIW horn antenna mounted on a large conducting plane," *IEEE Trans. Antennas Propag.*, vol. 62, no. 11, pp. 5895–5900, Nov. 2014.

[11] N. Bayat-Makou and A. A. Kishk, "Back radiation suppression for substrate integrated H-plane horn antenna," in *Proc. Int. Conf. IEEE Ubiquitous Wireless Broadband*, Montreal, QC, Canada, Oct. 2015, pp. 1–3.

[12] Y. Cai, Y. Zhang, Z. Qian, W. Cao, and L. Wang, "Design of compact air-vias-perforated SIW horn antenna with partially detached broad walls," *IEEE Trans. Antennas Propag.*, vol. 64, no. 6, pp. 2100–2107, Jun. 2016.

[13] N. Bayat-Makou and A. A. Kishk, "Substrate integrated horn antenna with uniform aperture distribution," *IEEE Trans. Antennas Propag.*, vol. 65, no. 2, pp. 514–520, Feb. 2017.